Arch. Metall. Mater. **63** (2018), 3, 1173-1178

DOI: 10.24425/123790

M. KRUPIŃSKI*#

EFFECT OF ADDITION Ce ON CRYSTALLISATION KINETICS AND STRUCTURE OF Zn-Al-Cu ALLOYS

The main goal of the presented work was to determine the relationship between changes in the shape of the derivative curve and the microstructure of Zn-Al-Cu alloys before and after modification. To describe the phenomena that occur in the material during solidification as a result of the modification in the chemical composition, the thermal-derivative analysis method was applied. This method allows to describe and interpret the kinetics of crystallisation of the tested alloys. To describe the morphology and phase composition, light and electron microscopy (SEM, TEM) was also used.

The modification of the hypereutectic Zn-Al-Cu alloys with the addition of Ce causes a reduction in the size $\alpha' + \eta$ eutectics and change in the morphology of the α' phase precipitates from dendritic to "tweed".

Keywords: casting alloys, crystallisation kinetics, Zn-Al alloy, Ce modification

1. Introduction

The appropriate use of the crystallisation mechanisms that enable the manufacturing of casts with optimum microstructure and properties is an essential factor in the improvement of the quality of cast products. It is well known that zinc-aluminium and aluminium-zinc based foundry alloys, especially the sand-cast ones, solidify naturally with coarse dendritic structure, which detrimentally influences plastic properties. Therefore they are grain-refined by small addition of, mainly, Ti, B or RE, added usually together with Al or Zn-matrix master alloys [1]. The properties of Zn-Al alloys are mainly due to the morphology of phase α'. Therefore, alloying elements are introduced into the alloys, which modify this phase. On the other hand, the low melting point of zinc alloys and the unfavorable effect of overheating on their properties require the application of modifications at lower temperatures [2].

In the case of casting alloys, a crystallisation process is conducted in temperatures between the liquidus and solidus ones, which mainly depend on the alloy composition, cooling rate and thermodynamic conditions of a transformation. The free energy values for liquid and solid phases depend on the concentration of alloy components. Crystallization driving force for alloys is the difference between the free energy of a liquid and the energy of a solid-liquid phase mixture in the concentration range of the components for a solid-liquid phase [3-8]. Copper influences the increase in strength, hardness and corrosion resistance. Also, copper causes a shift of the eutectic point in the Zn-Al-Cu alloy towards higher aluminum concentration. The addition of copper causes the free aging of Zn-Al alloys. This has little effect on the eutectoid reaction phase $\alpha(\alpha')$ and changes in solubility in a solid state in a low temperature range, but primarily on solid phase transformations involving the hexagonal η phase, the regular and wall-centred $\alpha(\alpha')$ phase, the hexagonal ε phase (Zn_4Cu), and the hexagonal τ phase (the Zn_3Cu intermetallic compound). The phase τ crystallises in a 0.6-0.7% Cu mass concentration range in an alloy and causes significant dimensional changes of casts [9-11].

Applying Ce as a modifier of microstructure at the level 0.8% related to mass causes significant fragmentation of the microstructure components also due to the increased fragmentation of the dendrite α phase. It has been stated that Ce does not dissolve in the matrix, but it forms intermetallic inter alia Al_4Ce phases in dendritic areas [12]. The crushing of structural components and an increase of mechanical properties for Al-Zn-Mg-Cu alloys were confirmed for 0.2 to 0.4% mass Ce content. The additive of Ce causes both modifications of grains and eutectic solidification of an alloy, as well as fosters separation of the η' phase. Furthermore, the Ce causes deformation of the system due to the difference between atomic diameters of Ce (0.27nm) and Al (0.128 nm) [13].

The RE additive has an influence on increasing the properties and corrosion resistance of Zn alloys [14]. The intermetallic phases of La and Ce cause a decrease in oxygen cathodic reduction and the formation of a passive layer, which leads to further anodic reduction of corrosion [15].

* SILESIAN UNIVERSITY OF TECHNOLOGY, INSTITUTE OF ENGINEERING MATERIALS AND BIOMATERIALS, 18A KONARSKIEGO ST., 44-100 GLIWICE, POLAND

Corresponding author: Mariusz.Krupinski@polsl.pl

2. Research methodology

The thermal analysis of the alloys tested, the chemical composition of which is given in Table 1 was performed on a UMSA MT5 device. Samples measuring ø30×35 mm intended for thermal research were prepared from the previously formed experimental smelting and they were melted in a graphite crucible. K-type thermocouples were placed in the same location (a district heating substation), whose position had been determined during the initial tests. The cooling rate was ~0,1°C/s for freely cooling samples (for the given system and the weight of the sample). The samples were cooled by using pressurised argon gas supplied by nozzles made in the drive to force an appropriately higher experimentally established cooling rate. The intensity of the flowing cooling gas of the sample was adjusted by a rotameter. Micro-sections prepared were etched in reagents: 10% HF, and 10 gCrO_3 + 1 gNa_2SO_4 + 200 ml H_2O, then were rinsed in 40 gCO_3 + 200 ml H_2O. Metallographic examinations were performed using the Leica MEF 4A metallographic microscope, Zeiss Axio Observer, Olympus LEXT OLS4000 using a computer image analysis system at 50 to 500× magnifications. To allow a comparison of the analysis results of the tested alloy structures, parameters which characterise all the structures of the alloys tested were measured i.e. the circumference and the surface of structural components containing Al as the main component. The ratio of the surface to the circumference is a measure of the fragmentation of structural components. Analysis of the microstructure of thin foils and phase identification of the precipitates were made utilising transmission electron microscope (TEM) JEOL 3010CX, at accelerating voltage of 300 kV using electron diffraction to identify phase components.

TABLE 1

Chemical composition of tested zinc alloys

No. alloy	Mass concentration of alloying elements in tested alloys, %			
	Al	Cu	Ce	Zn
1	10.02	0.98	—	Residue
2	9.6	0.78	0.078	Residue
3	8.04	0.64	0.68	Residue

3. Results of the thermal-derivative analysis

A representative cooling curve of crystallisation of the Zn-Al-Cu alloy cooled at 0.1°C · s^{-1} in the temperature range of 450°C to 350°C is shown in Figure 1. Analysing the crystallisation process based on the obtained curves of the temperature changes and the derivative dT/dt, it was found that the α phase nucleation process (at the point of inflexion I) begins in the temperature T_L. Admittedly, the thermal effects accompanying the nucleation and growth process of α crystals provide additional heat to the forming liquid and solid phase mixture, however, the heat balance of the cooling cast ingot is negative. The chemical composition of the remaining liquid changes according to the liquid line of the Zn-Al graph. In this range, the approximately constant value of the dT/dt derivative is observed. The liquid is enriched more and more with zinc and nucleation of eutectic $\alpha + \eta$. As a result of further cooling, the remaining liquid crystallises theoretically at a constant temperature $T_{E(Al+Zn)}$ ($dT/dt = 0$) to form $\alpha + \eta$ eutectic (point II). Crystallization ends when the alloy reaches the T_{Sol} temperature. In experimental practice, the temperature characteristic of the beginning and the end of the eutectic transformation has a little difference, and it is assumed that the temperature of the solidus T_{Sol} is the temperature corresponding to the point III in Figure 1 (the eutectic solidification end, Table 2). As a result of the analysis of the thermodynamic parameters, the corresponding values of the C_{pl} heat capacity in a liquid state and the C_{ps} heat capacity in a solid state were determined for the Zn-Al-Cu alloy as shown in Table 3. The results of the calculation of the latent heat of crystallisation of the components of the alloys tested as well as their percentage was reported.

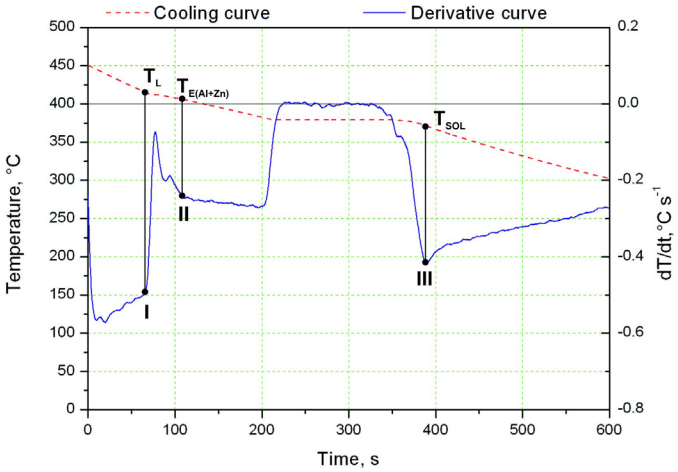

Fig. 1. Cooling curve and derivative curve for the Zn-Al-Cu alloy cooled at a rate of 0.1°C · s^{-1}

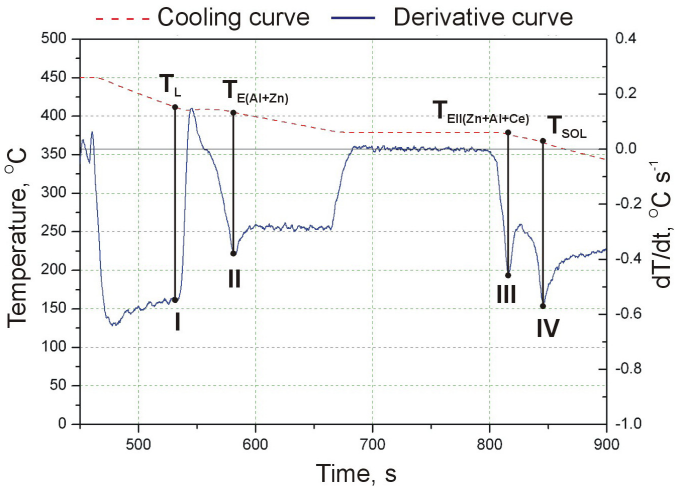

Fig. 2. Cooling curve and Derivative curve for the Zn-Al-Cu alloy cooled at a rate of 0.1°C · s^{-1} with 0.68% mas. Ce

Unlike the non-modified alloys, in alloys containing cerium, characteristic thermal changes indicating the formation of a mul-

TABLE 2

Characteristic temperature of the particular stages of phase transformation during crystallisation of Zn-Al-Cu alloy

Type of alloy	Temperature °C	
	T_L	T_{Sol}
Cooling rate 0.1°C/s		
Zn-Al-Cu	414.5	372.7
Zn-Al-Cu-Ce (0.078% mas. Ce)	401.8	370.4
Zn-Al-Cu-Ce (0.68% mas. Ce)	409.5	368.1

TABLE 3

Latent heat crystallization generated by crystallizing phases and its percentage in the total heat of crystallization of Zn-Al-Cu alloys cooled at $0.1°C \cdot s^{-1}$

Heat capacity in liquid state Cp_l, J/g×°C	Heat capacity in solid state Cp_s, J/g×°C		Weight of sample, g
0.5305	0.4407		152.08
Reaction	Latent heat of crystallization		Percentage %
	Samples J	Unit weight of a sample, J/g	
$L \rightarrow \alpha$	576.73	3.79	7.63
$L \rightarrow E_{(\alpha+\eta)}$	6723.56	44.21	92.37
Total	7300.29	48.00	100

ticomponent eutectics rich in cerium (Fig. 2, point III), whose crystallization starts at $T_{EII(Al+Zn+Ce)}$ and lasts until the solidus T_{Sol} temperature (point IV) is reached, can be determined in the course of the crystallisation process.

At a temperature 450°C with a sufficiently long melting time, the cerium goes into the solution and solidifies probably as the last component in the form of multi-component eutectics (point III in Fig. 2). It is worth emphasising that the modification of the Zn-Al-Cu alloy by the use of cerium causes an reduction in the solidification temperature of the α phase, as well as the reduction of the crystallization stage temperature of the T_{Sol} alloy (Table 2).

The change in the shape of the derivative curve may result from the character of the transition between the crystallisation of individual phases and eutectics and is related to the cooling rate and chemical composition.

In Table 4 the calculated values of heat capacity in a liquid state C_{pl}, heat capacity in a solid state C_{ps}, latent heat of crystallisation of alloy components and their percentage have been correlated.

3. Structural research results

The structural studies complemented an analysis of the effects of phase transformation during crystallisation of alloys. The results of metallographic studies conducted using light microscopy that the over-eutectic zinc alloys of aluminum and copper are characterized by the structure of the α' (aluminum zinc solution) solid solution and the $\alpha'+\eta$ eutectic grains, without Cu-rich ε phase separation (solid solution of Cu in Zn), whose

TABLE 4

Latent heat of crystallization generated by crystallising phases and its percentage in the total crystallisation heat of Zn-Al-Cu-Ce (0.078% mas.Ce) cooled at $0.1°C \cdot s^{-1}$

Heat capacity in liquid state, Cp_l, J/g×°C	Heat capacity in solid state Cp_s, J/g×°C		Weight of sample, g
0.5289	0.44076		152.18
Reaction	Latent heat of crystallization		Percentage, %
	Samples J	Unit weight of a sample, J/g	
$L \rightarrow \alpha$	281.27	1.85	3.41
$L \rightarrow E_{(\alpha+\eta)}$	7163.98	47.08	93.88
L → α+η+Ce	188.26	1.24	2.71
Total	7633.51	50.17	100

morphology depends on the cooling rate used. Examples of microstructure images, which are composed of the globulins of precipitation of "fine eutectics" and eutectics $\alpha'+\eta$, with morphology dependent on cooling conditions.

It was found that the addition of cerium resulted in the formation of a "tweed" microstructure (Fig. 3b). The Zn_2Ce and Zn_3Ce phases are also visible in the eutectic $\alpha'+\eta$ (Fig. 4).

The use of the image analysis of metallographic structures allowed to compare the changes in the size of the structural components compared to the Zn-Al alloy. Visible fragmentation of the fine eutectic precipitation, as well as smaller values of the surface and the circumference, indicate decreasing of α' precipitation in the eutectic.

At 275°C, a eutectoid transformation takes place, the beginning and the end of reaction shift the alloy additions [16]. As a result of solid state diffusion transformation in the eutectoid reaction zone between α and η, a finer phase mixture α' and η forms (zone 4 in Fig. 5). Inside the primary grains (formed as a result of solidification) the diffusion of excess Zn occurs at very short distances and forms as very small "eutectic" areas (zone 2 in Fig. 5). The Ce addition changes the morphology of the primary phases as well as the diffusion in solid state transformation.

TABLE 5

The results of quantitative WDS analysis of the chemical composition of Zn-Al-Cu alloy with the Ce addition, cooling rate $0.1°C \cdot s^{-1}$ (Fig. 5)

Point of analysis	The mass concentration of the element in the alloy, %	
	Al	Zn
1	1.4	98.6
2	36.5	63.5
3	39.4	60.6
4	19.9	80.1
5	39.3	60.7

Studies using high-resolution transmission electron microscope confirmed that the resulting cerium-enriched alloys are characterised by a marked polycrystalline structure in which the grain size is in the range from 15 nm to 10 μm often showing significantly defected area network structure – with different

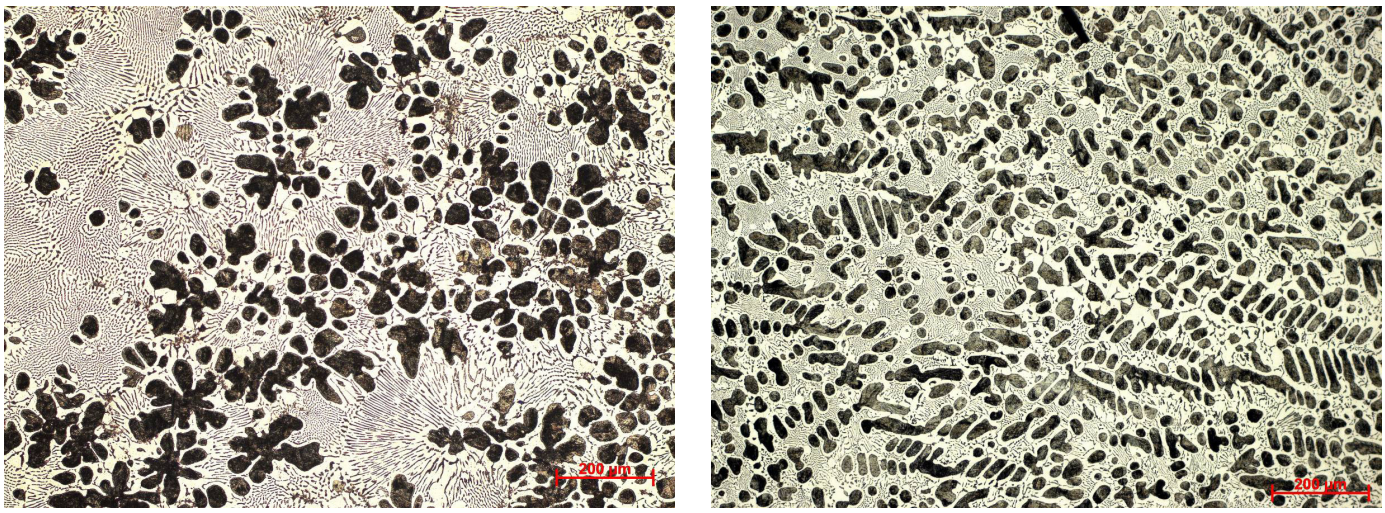

a) b)

Fig. 3. Microstructure of Zn-Al-Cu, cooling rate 0.1°C · s^{-1}: a) without modification, b) with 0,68% mas. Ce

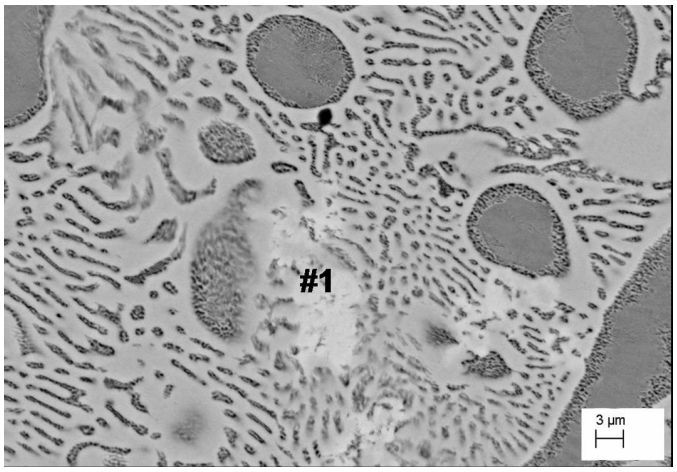

Fig. 4. Microstructure of Zn-Al-Cu-Ce with 0,68% mas.Ce, cooling rate 1°C · s^{-1}; #1 – phase with Ce

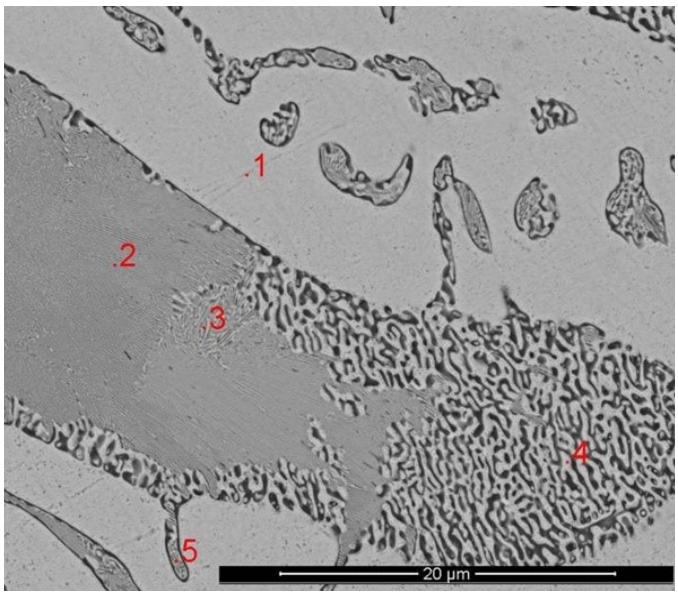

Fig. 5. Microstructure of Zn-Al-Cu cast alloy with Ce addition, cooling rate 0.1°C/s

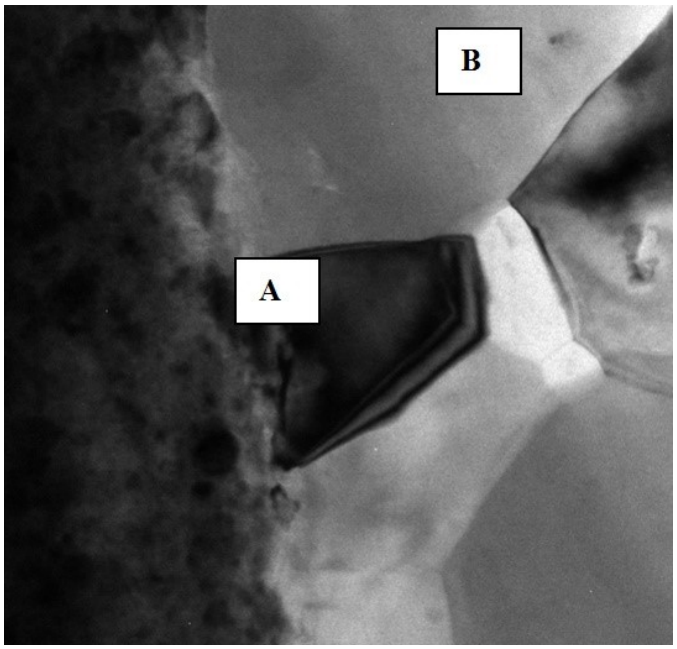

Fig. 6. Microstructure of Zn-Al-Cu alloys with Ce addition, grain boundary, bright field, TEM analysis

dislocation density. Using energy dispersive spectrometer in the structure of the Zn-Al-Cu alloy with Ce addition, the occurrence of precipitates from the Ce was confirmed. The precipitates containing cerium occur in the test alloy not only as individual particles, but also as conglomerates of this phase with different spatial orientation.

Diffraction studies performed in the form of the electron diffraction patterns made it possible to confirm the fine-grained polycrystalline structure of the tested alloy allowing identification of the Zn_{α} substrate phase.

Figure 6 shows the nature of the transition zone between grains with a significant difference in dislocation density. These zones are characterised by a smooth transition with a visible boundary between the area with a significant dislocation density

(mark #A in Fig. 6) and grains with a relatively homogeneous crystalline structure without defects (mark #B in Fig. 6). Performed analyses presented in earlier works, eg [16] confirm the presence of Zn_2Ce phases in the structure [0 3 $\bar{1}$] and Zn_3Ce [4 3 $\bar{4}$] (Fig. 7 and 8).

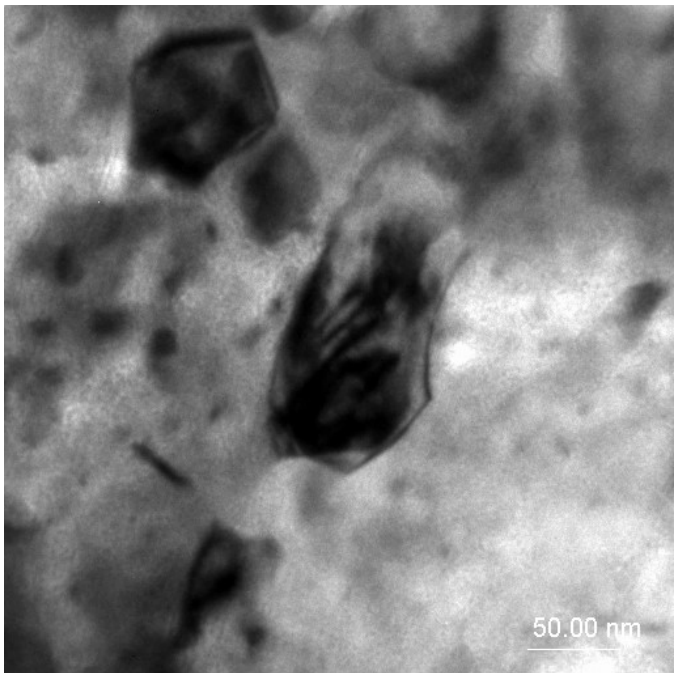

Fig. 7. Microstructure of Zn-Al-Cu alloy with Ce addition with visible Zn_3Ce phase, bright field, TEM analysis

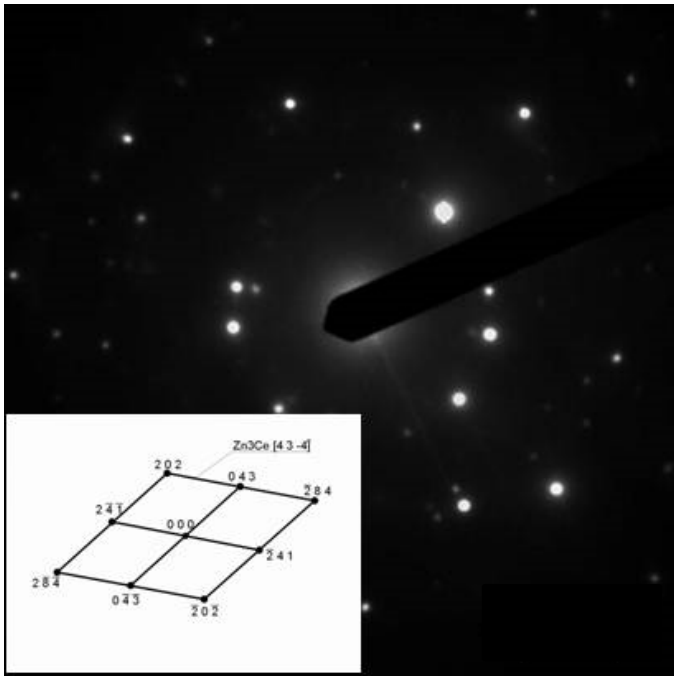

Fig. 8. The diffractogram from the area in Figure 7 with the Zn_3Ce solution, axis zone [4 3 $\bar{4}$]

4. Conclusions

The cooling rate and the element in the form of Ce also affect on the fraction solid depending on the temperature of the solidifying alloy. It was found that changes in the cooling rate in the range from 0.1 to 1°C·s^{-1} do not cause changes in the phase composition of the tested alloys, but only changes in the morphology of aluminum precipitates and $\alpha' + \eta$ eutectic as well as grain size and distance of eutectic plates. Changing the cooling rate results in a decreasing of the temperature at the end of the crystallisation of the alloy, thereby increasing the temperature range of solidification of the alloy. The analysis of eutectics allows noticing its two natures. The first class as coarse form of eutectics arises during crystallisation and the second class ("fine eutectic"), with a more significant fragmentation of the components, is probably the result of steady-state transformation as a result of diffusion (eutectoid transformation). The content of Cu in the alloy could indicate the possibility of phase ε formation, but as a result of research, no such phases were found, and copper occurs in the form of a solution in the matrix. Addition of a modifier causes a shift in the temperature of the beginning and the end of the eutectoid transformation.

The modification by Ce addition in the zinc alloy changes the microstructure. The analysis of the microstructure of analysed alloys confirmed the precipitations containing aluminum, the $\alpha' + \eta$ eutectic and the formation of Zn_2Ce [16] and Zn_3Ce phases that are compounds of multi-component eutectics. The Ce addition causes that the microstructure takes the form of "tweed". The modification by Ce element into the melt causes a change in nucleation temperature of α phase and the end of crystallisation process of the alloy.

Acknowledgements

This publication was financed by the Ministry of Science and Higher Education of Poland as the statutory financial grant of the Faculty of Mechanical Engineering SUT.

REFERENCES

[1] W.K. Krajewski, J. Buras, P.K. Krajewski, A.L. Greer, K. Faerber, Mater Today-Proc. **2**, 4978-4983 (2015).

[2] W.K. Krajewski, Research of the heterogeneous nucleation mechanism in high-aluminium zinc alloys modified by Ti addition, Wyd. AGH (1996) in Polish.

[3] L. Arnberg, L. Bäckerud, A. Dahle, Castability of Aluminium Foundry Alloys, AFS Research Report, Illinois 1999.

[4] E. Fras, W. Kapturkiewicz, A. Burbelko, H.F. Lopez, A New Concept in Thermal Analysis of Castings, AFS Transactions 101, 1993.

[5] W.T. Kierkus, J.H. Sokolowski, Recent Advances in Cooling Curve Analysis: A New Method for determining the 'Base Line' Equation, AFS Transactions 107, 1999.

[6] M. Krol, T. Tanski, P. Snopinski, B. Tomiczek, J. Therm. Anal. Calorim. **127** (1), 299-308 (2017)

[7] M. Krol, T. Tanski, W. Sitek, Adv. Mate.r Res-Switz. **95**, Art. Nr. 012006. (2015).

[8] M. Krupinski, B. Krupinska, K. Labisz, Z. Rdzawski, T. Tanski, Proc. Inst. Mech. Eng. Part L-J. Mat.-Des. Appl. **230**/3: 805-812 (2016).

[9] A.E. Ares, L.M. Gassa, S.F. Gueijman, C.E. Schvezov, J. Cryst. Growth. **3101**, 355-1361 (2008).

[10] M. Durman, S. Murphy, J. Mater. Sci. **32**,1603-1611 (1997).

[11] W.K. Krajewski, A.L. Greer, P.K. Krajewski, Arch. Metal. Mater. **58**, 845-847 (2013).

[12] S.F. Liu, B. Li, X.H. Wang, W. Su, H. Han, J. Mater. Process Tech. **209**, 3999-4004 (2009).

[13] J.P. Lai, R.P. Jiang, H.S. Liu, X.L. Dun, Y.F. Li, X.Q. Li, J. Cent. South Univ. **19**, 869-874 (2012).

[14] D. Veys-Renaux, K. Guessoum, E. Rocca, N. David, K. Belhamel, Corr. Sci. **77**, 342-349 (2013).

[15] D. Veys-Renaux, K. Guessoum, E. Rocca, N. David, K. Belhamel, Corr. Sci. **77**, 342-349 (2013).

[16] M. Krupiński, B. Krupińska, Z. Rdzawski, K. Labisz, T. Tański, J. Therm. Anal. Calorim. **120**/3, 1573-1583 (2015).